An accepted version of Mäkelä et al., Water Res 91 (2016) 11-18, available at:
http://dx.doi.org/10.1016/j.watres.2015.12.043.

Predicting the drying properties of sludge based on hydrothermal treatment under subcritical conditions

Mikko Mäkelä*[a], Laurent Fraikin[b], Angélique Léonard[b], Verónica Benavente[c], Andrés Fullana[c]

[a] Swedish University of Agricultural Sciences, Department of Forest Biomaterials and Technology, Skogsmarksgränd, 90183 Umeå, Sweden

Current address: Tokyo Institute of Technology, Department of Environmental Science and Technology, G5-8, 4259 Nagatsuta-cho, Midori-ku, Yokohama 226-8502, Japan

[b] University of Liège, Department of Chemical Engineering, Agora, B6c, Allée du 6 Août, 4000 Liège, Belgium (L. Fraikin: laurent.fraikin@ulg.ac.be, A. Léonard: a.leonard@ulg.ac.be)

[c] University of Alicante, Department of Chemical Engineering, P.O. Box 99, 03080 Alicante, Spain (V. Benavente: veronica.benavente@ua.es, A. Fullana: andres.fullana@ua.es)

*corresponding author, tel.: +81 (0)45 924 5507, fax: +81 (0)45 924 5507, email: makela.m.aa@m.titech.ac.jp, mikko.makela@slu.se

An accepted version of Mäkelä et al., Water Res 91 (2016) 11-18, available at:
http://dx.doi.org/10.1016/j.watres.2015.12.043.

Abstract

The effects of hydrothermal treatment on the drying properties of sludge were determined. Sludge was hydrothermally treated at 180-260 °C for 0.5-5 h using NaOH and HCl as additives to influence reaction conditions. Untreated sludge and attained hydrochar samples were then dried under identical conditions with a laboratory microdryer and an X-ray microtomograph was used to follow changes in sample dimensions. The effective moisture diffusivities of sludge and hydrochar samples were determined and the effect of process conditions on respective mean diffusivities evaluated using multiple linear regression. Based on the results the drying time of untreated sludge decreased from approximately 80 minutes to 37-59 minutes for sludge hydrochar. Drying of untreated sludge was governed by the falling rate period where drying flux decreased continuously as a function of sludge moisture content due to heat and mass transfer limitations and sample shrinkage. Hydrothermal treatment increased the drying flux of sludge hydrochar and decreased the effect of internal heat and mass transfer limitations and sample shrinkage especially at higher treatment temperatures. The determined effective moisture diffusivities of sludge and hydrochar increased as a function of decreasing moisture content and the mean diffusivity of untreated sludge ($8.56 \cdot 10^{-9}$ m^2 s^{-1}) and sludge hydrochar ($12.7\text{-}27.5 \cdot 10^{-9}$ m^2 s^{-1}) were found statistically different. The attained regression model indicated that treatment temperature governed the mean diffusivity of hydrochar, as the effects of NaOH and HCl were statistically insignificant. The attained results enabled prediction of sludge drying properties through mean moisture diffusivity based on hydrothermal treatment conditions.

Keywords: Biosolids; Moisture diffusivity; Hydrochar; Hydrothermal carbonization; Shrinkage; X-ray microtomography

An accepted version of Mäkelä et al., Water Res 91 (2016) 11-18, available at:
http://dx.doi.org/10.1016/j.watres.2015.12.043.

1. Introduction

Handling of sludge residues generated by biological and chemical wastewater treatment is becoming ever more challenging due to rapid urbanization and increasing efficiency requirements for municipal and industrial wastewater treatment plants. Sludge residues are widely complex materials due to a variety of structural components such as extracellular polymeric structures, filamentous bacteria, cationic salts and the potential presence of pollutant precursors, e.g., proteins and fats, pathogens, parasites, trace metals, polychlorinated biphenyls, dioxins and other slowly decomposable compounds (Vaxelaire and Cézac, 2004; Yoshikawa and Prawisudha, 2014b). Currently the most common sludge handling methods include incineration, composting, use in agriculture or disposal in landfills (Mahmood and Elliott, 2006; Mowla et al., 2013), although current trends in European regulation are increasingly hindering landfill deposition of organic substances. As sludge is an inherently wet material decreasing associated handling, storage and transportation costs generally requires active drying especially for smaller-scale treatment plants. However current means of mechanical dewatering suffer from difficulties in removing intracellular and chemically bound water from the polymeric matrix of sludge suspensions (Mowla et al., 2013; Stoica et al., 2009).

Hydrothermal treatment performed with water acting as a solvent, a reactant and even a catalyst or catalyst precursor does not require prior drying of a sludge feedstock and allows simultaneous elimination of biologically active organisms or compounds (Peterson et al., 2008). Hydrothermal treatment under subcritical conditions can be used for producing carbonaceous hydrochar with relatively high yields (Libra et al., 2011) and enables the conversion of non-traditional feedstock such as municipal and industrial sludge residues. The increasing ion product of water under hydrothermal conditions typically favours reactions which are catalysed by acids or bases and is generally understood to proceed via a network of hydrolysis, dehydration, decarboxylation, polymerization and aromatization of biomass components (Kruse et al., 2013; Sevilla and Fuertes, 2009). As hydrothermal treatment is ideally operated under saturated steam pressure the latent heat requirement of evaporation can also be avoided although post-separation of solid and liquid phases is still required. Irrespective of potential hydrochar applications such as direct solid fuel replacement, soil amelioration or metal/metalloid adsorption (Alatalo et al., 2013; Libra et al., 2011; Titirici and Antonietti, 2010), elimination of hydroxyl and carboxyl groups followed by subsequent aromatization can enhance the drying properties of sludge due to increased hydrophobicity and sludge cell breakage (Wang et al., 2014; Yoshikawa and Prawisudha, 2014a; Zhao et al., 2014b).

The drying properties of a material are conveniently characterized through the drying curve where drying rate is described as a function of drying time under specific drying conditions. The attained drying curve allows the identification of controlling mechanisms such as moisture evaporation from

saturated or unsaturated surfaces or diffusion within a material (Mujumdar, 2007). In addition, effective moisture diffusivity can be used for compiling empiric drying data to a single parameter describing moisture transfer independent of the actual mechanisms involved (Gómez-de la Cruz et al., 2015). Although diffusivity coefficients are often determined through a simplification of Fick's second law of diffusion, reliable estimations for non-rigid materials can only be attained if material shrinkage is taken into account (Bennamoun et al., 2013). Non-extrusive imaging techniques such as X-ray microtomography have been shown to provide detailed quantitative information on material shrinkage and thus enable a better understanding of the relationships between drying properties and the evolution of size and shape (Léonard et al., 2004; Léonard et al., 2008).

For reliably determining the effect of hydrothermal treatment on the drying properties of sludge, we illustrate the use of X-ray microtomography for monitoring sample shrinkage during drying of sludge and hydrochar samples. Respective effective moisture diffusivities affected by shrinkage were then determined by applying recent developments on the interpretation of experimental drying data. Finally, the effect and statistical significance of treatment conditions such temperature, retention time and additive quality on the mean moisture diffusivity of hydrochar were determined using multiple linear regression. The attained results help in understanding the effect of process conditions on the drying properties of hydrothermally treated sludge and controlling these properties based on treatment conditions.

2. Material and methods

2.1 Sampling and sample preparation

Sludge samples were attained from a Swedish pulp and paper mill using virgin sulphate and recycled fibre pulp for the production of unbleached kraft/euroliner for corrugated cardboard. Mill effluents were treated by primary gravitational settling followed by biological activated sludge treatment. Approximately 300 kg of mixed sludge (containing 60% of primary sludge and 40% of biosludge) was sampled after primary sludge and surplus biosludge from secondary sedimentation had been mixed and dewatered to approximately 27% dry solids (2.7 kg H_2O kg^{-1} db, dry basis) using a belt filter and a centrifuge at the mill. The 300 kg sample was coned and quartered (Gerlach et al., 2002) to a representative 10 kg subsample which was stored in +4 °C during the experiments.

2.2 Hydrothermal treatment

Hydrothermal experiments were performed with a 1 L non-stirred stainless steel reactor (Amar Equipments PVT Ltd., Mumbai, India) illustrated Fig. 1a. A constant 300 g mass of sampled sludge was thoroughly mixed with 75 mL of additive and loaded into the reactor. The reactor was heated to

reaction temperature using a 1.5 kW electric heating resistance and an additional heating plate placed under the reactor. The 1.5 kW heating resistance was PID controlled as the additional heating plate was set to reaction temperature. Reactor pressure was indicated by a pressure gauge and was approximately equivalent to saturated vapour pressure of water under respective reaction temperatures (i.e., 1-5 MPa). As the isothermal retention time was complete, the reactor was cooled with pressurized air and the gases released into a fume hood. The solid and liquid phases were subsequently separated by vacuum filtration through a grade 413 VWR® filter paper (VWR International LLC, Radnor, PA, USA).

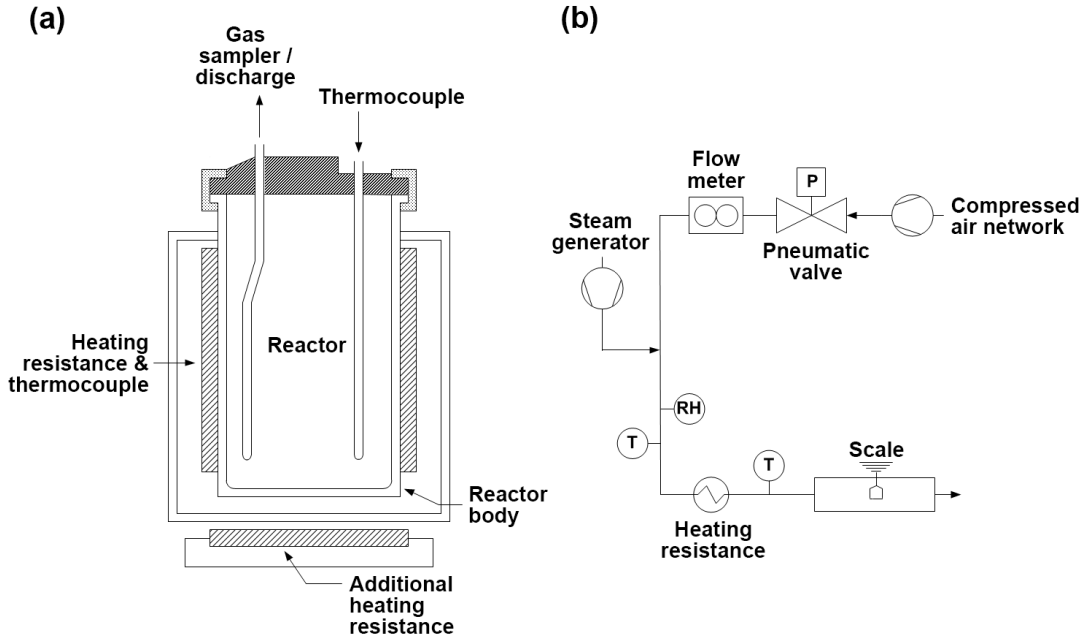

Fig. 1: Schematic presentations of a) the hydrothermal reactor and b) the microdryer.

The experiments were conducted according to an experimental design including reaction temperature (180-260 °C) and log10 transformed retention time (0.5-5 h) as continuous controlled variables. In addition, additive type was included as a discrete variable to influence reaction conditions by mixing 75 mL NaOH (0.01 N, pH 12.1) or HCl (0.01 N, pH 2.5) with the feed material prior to loading into the reactor. Deionized H_2O was used as a control (conductivity <6 mS cm^{-1}) and both NaOH and HCl used for making the solutions were reagent grade. NaOH was chosen as it is commonly used in the chemical recovery cycles of pulp mills and the inclusion of HCl enabled evaluating the effect of a wider pH range. Additive concentrations were chosen based on Lu et al. (2014) and the final solid load adjusted to remain in the range applicable to dewatered sludge within the pulp and paper industry. As the design included a discrete variable it was constructed to allow the use of dummy variables in linear regression and response surface methodology (Myers et al., 2009). The final design (see Table 1) was composed of 15 individual experiments.

An accepted version of Mäkelä et al., Water Res 91 (2016) 11-18, available at:
http://dx.doi.org/10.1016/j.watres.2015.12.043.

Table 1: Hydrothermal treatment conditions and mean moisture diffusivities of hydrochar.

Exp. n:o	Reaction temperature (°C)	Retention time		Additive	Determined mean effective diffusivity (10^{-9} m^2 s^{-1})[a]
		h	log h		
1	180	0.50	-0.3	NaOH	12.7
2	260	0.50	-0.3	NaOH	17.9
3	180	5.00	0.699	NaOH	13.9
4	260	5.00	0.699	NaOH	27.5
5	180	1.58	0.1995	NaOH	13.6
6	220	5.00	0.699	NaOH	18.1
7	180	0.50	-0.3	H_2O	14.8
8	260	0.50	-0.3	H_2O	18.2
9	180	5.00	0.699	H_2O	16.4
10	260	5.00	0.699	H_2O	23.8
11	180	0.50	-0.3	HCl	13.2
12	260	0.50	-0.3	HCl	16.7
13	180	5.00	0.699	HCl	17.0
14	260	5.00	0.699	HCl	18.9
15	220	1.58	0.1995	HCl	14.7

[a] Mean effective moisture diffusivity of untreated sludge $8.56 \cdot 10^{-9}$ m^2 s^{-1}

2.3 Drying experiments and X-ray microtomography

Prior to drying the individual sludge and hydrochar samples were shaped to ensure comparability of initial stress states. The samples were compressed for 1 minute under 50 N in a cylindrical compression cell (Ø 20 mm) consisting of a movable piston and a closed grid that allowed water to be removed. The obtained cylindrical samples were then cut to lengths equivalent to 4.10 ± 0.041 g in sample mass. The corresponding sample volumes were hence dependent on the specific properties of sludge or hydrochar.

Drying experiments were performed with a laboratory micro-dryer by following sample mass loss under constant and reproducible drying conditions, Fig. 1b (Léonard et al., 2002). The prepared samples were inserted to a drying chamber (cross-section 41 × 46 mm) on a grid suspended under a precision scale to allow convective drying on the entire external surface. The mass of the samples were then recorded every 5 seconds under an air velocity of 1.5 m s^{-1}, a temperature of 105 °C and an absolute humidity of 0.007 kg H_2O kg^{-1} dry air. Drying was continued until no further changes in sample mass were observed and the dried samples placed into an oven at 105 °C to determine respective dry solids contents according to standard methods. The mass loss signals were then preprocessed by excluding data points above 95% dry solids (0.053 kg H_2O kg^{-1} db) for removing interferences at low moisture contents.

An accepted version of Mäkelä et al., Water Res 91 (2016) 11-18, available at:
http://dx.doi.org/10.1016/j.watres.2015.12.043.

External surface areas and sample volumes were calculated based on image analysis by X-ray microtomography. Each sample was scanned before and after drying (Fig. 2) with a 1074 portable X-ray micro-CT scanner (Skyscan, Kontich, Belgium) for 3 minutes resulting in 105 projections. Each sample was tilted around 180° recording one projection every 1.7° for minimization of acquisition time. Sample masses were also measured before and after tomography for linking external surface areas and sample volumes to respective moisture contents (Fraikin, 2012). Sample shrinkage was assumed linear in respect to sample moisture contents (Léonard et al., 2004; Li et al., 2014).

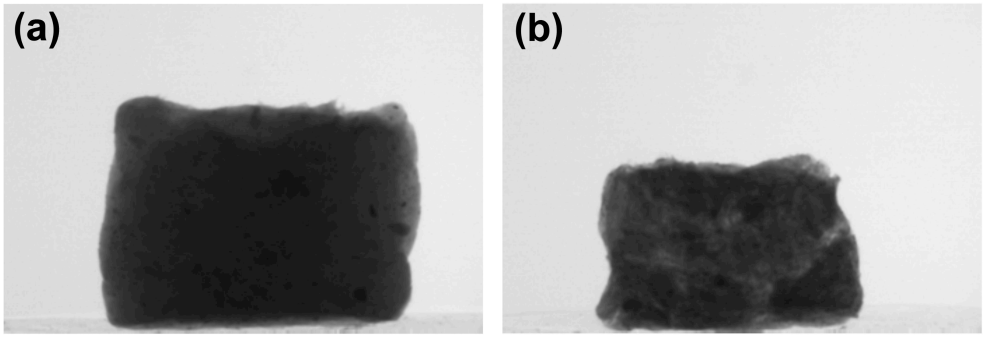

Fig. 2: Example X-ray images of untreated mixed sludge a) before and b) after drying.

3. Calculations

The drying fluxes of sludge and hydrochar samples were calculated by correcting the recorded drying data with the external surface area of each sample from X-ray imaging. In addition, respective sample volumes were calculated. Raw drying data was also interpreted based on Fick's second law of diffusion on the hypothesis that moisture transfer was proportional to the concentration gradient of desorption (Bennamoun et al., 2013):

$$\frac{\partial X}{\partial t} = D_{eff,x} \cdot \frac{\partial^2 X}{\partial x^2} + D_{eff,y} \cdot \frac{\partial^2 X}{\partial y^2} + D_{eff,z} \cdot \frac{\partial^2 X}{\partial z^2} \quad (1)$$

where X denotes moisture content (kg H_2O kg^{-1} db), t drying time (s), D_{eff} the effective diffusivity (m^2 s^{-1}) and x, y and z the spatial dimensions of moisture transport (m). For short cylinders approaching a one-dimensional plane sheet with uniform initial moisture distribution Eq. (1) can be expressed as (Crank, 1975; Pacheco-Aguirre et al., 2014):

$$\phi = \frac{X(t)-X_e}{X_0-X_e} = \frac{8}{\pi^2} \sum_{n=0}^{\infty} \frac{1}{(2n+1)^2} \exp\left(-\frac{(2n+1)^2 \pi^2 D_{eff} t}{L^2}\right) \quad (2)$$

where ϕ describes dimensionless moisture ratio, X(t) moisture content (kg H_2O kg^{-1} db) at time t, X_e equilibrium moisture content approaching zero on longer drying times, X_0 the initial moisture content, n a positive integer and L sample height (m), i.e. sheet thickness. For considerable drying times Eq. (2) can be simplified by considering only the first term of the series, which becomes (Crank, 1975):

$$\frac{d}{dt}\ln\left(\frac{X(t)}{X_0}\right) = -\frac{D_{eff}\pi^2}{L^2} \quad (3)$$

Effective moisture diffusivity can then be determined through:

$$D_{eff} = -\frac{kL^2}{\pi^2} \quad (4)$$

where k is attained by derivating a polynomial function fitted to the experimental $\ln\left(\frac{X(t)}{X_0}\right)$ data.

The effects of controlled design variables, i.e. reaction temperature, retention time and additive quality, on the effective diffusivities of hydrochar were modelled through a multiple linear regression equation:

$$\mathbf{y} = \mathbf{Xb} + \mathbf{e} \quad (5)$$

where **y** represents a vector of determined mean diffusivities, **X** a coded and range-scaled design matrix including individual experiments as rows and experimental conditions as the respective columns, **b** a vector of model coefficients and **e** a residual vector. Model coefficients were determined by minimizing the sum of squares of model residuals through the least-squares fit:

$$\mathbf{b} = (\mathbf{X}'\mathbf{X})^{-1}\mathbf{X}'\mathbf{y}' \quad (6)$$

Individual model coefficients were refined by F-testing the variance explained by a coefficient against the variance of model residuals calculated as the difference between determined and predicted diffusivities:

$$\mathbf{e} = \mathbf{y} - \hat{\mathbf{y}} \quad (7)$$

where $\hat{\mathbf{y}}$ is a vector of predicted mean diffusivities:

$$\hat{\mathbf{y}} = \mathbf{Xb} \quad (8)$$

The effect of additive quality included as a discrete variable was determined through the use of two dummy variables c_1 and c_2 in the design matrix **X** where:

$$c_1 = \begin{matrix}1 \text{ if NaOH is the discrete level} \\ 0 \text{ elsewhere}\end{matrix} \quad (9)$$

An accepted version of Mäkelä et al., Water Res 91 (2016) 11-18, available at:
http://dx.doi.org/10.1016/j.watres.2015.12.043.

$$c_2 = \begin{matrix} 1 \text{ if HCl is the discrete level} \\ 0 \text{ elsewhere} \end{matrix} \quad (10)$$

The variation of determined diffusivities explained by the model was calculated through the R^2 value:

$$R^2 = 1 - \frac{SS_{res}}{SS_{tot}} \quad (11)$$

where SS_{res} denotes the sum of squares of model residuals and SS_{tot} the total sum of squares of **y** around the mean.

4. Results

A drying time of approximately 80 minutes was required to reach 95% dry solids in the untreated sludge sample and respectively decreased to a range 37-59 minutes for hydrothermally treated hydrochar. Time required for drying was accompanied by considerable sample shrinkage especially in the case of untreated sludge and was inversely correlated with hydrothermal treatment temperature ($p < 0.01$) and retention time ($p < 0.01$). The external surface area and volume of sludge and hydrochar samples assuming linear isotropic shrinkage were attained through X-ray tomography and used for calculating the drying flux as a function of sample moisture content. The results are provided in Fig. 3a and b.

The uncorrected drying data were further interpreted based on Fick's second law of diffusion in a one-dimensional plane sheet. Moisture ratio was first determined as a function of drying time (Fig. 3c) and the respective natural logarithm fitted with a second order polynomial (Fig. 3d). The attained polynomial coefficients represented a theoretical fit to the experimental data and were used together with respective sample heights (Fig. 3e) for determining the effective moisture diffusivity of sludge and hydrochar samples (Fig. 3f). As illustrated in Fig. 3f, the determined moisture diffusivities were inversely related to respective moisture contents during drying and thus increased towards the end of the drying experiments. The mean values of determined diffusivities of hydrochar were in the range $12.7\text{-}27.5 \cdot 10^{-9}$ m^2 s^{-1} (Table 1) and were found statistically different from the moisture diffusivity of untreated sludge ($8.56 \cdot 10^{-9}$ m^2 s^{-1}) on a $p < 0.01$ significance level according to a performed t-test.

An accepted version of Mäkelä et al., Water Res 91 (2016) 11-18, available at:
http://dx.doi.org/10.1016/j.watres.2015.12.043.

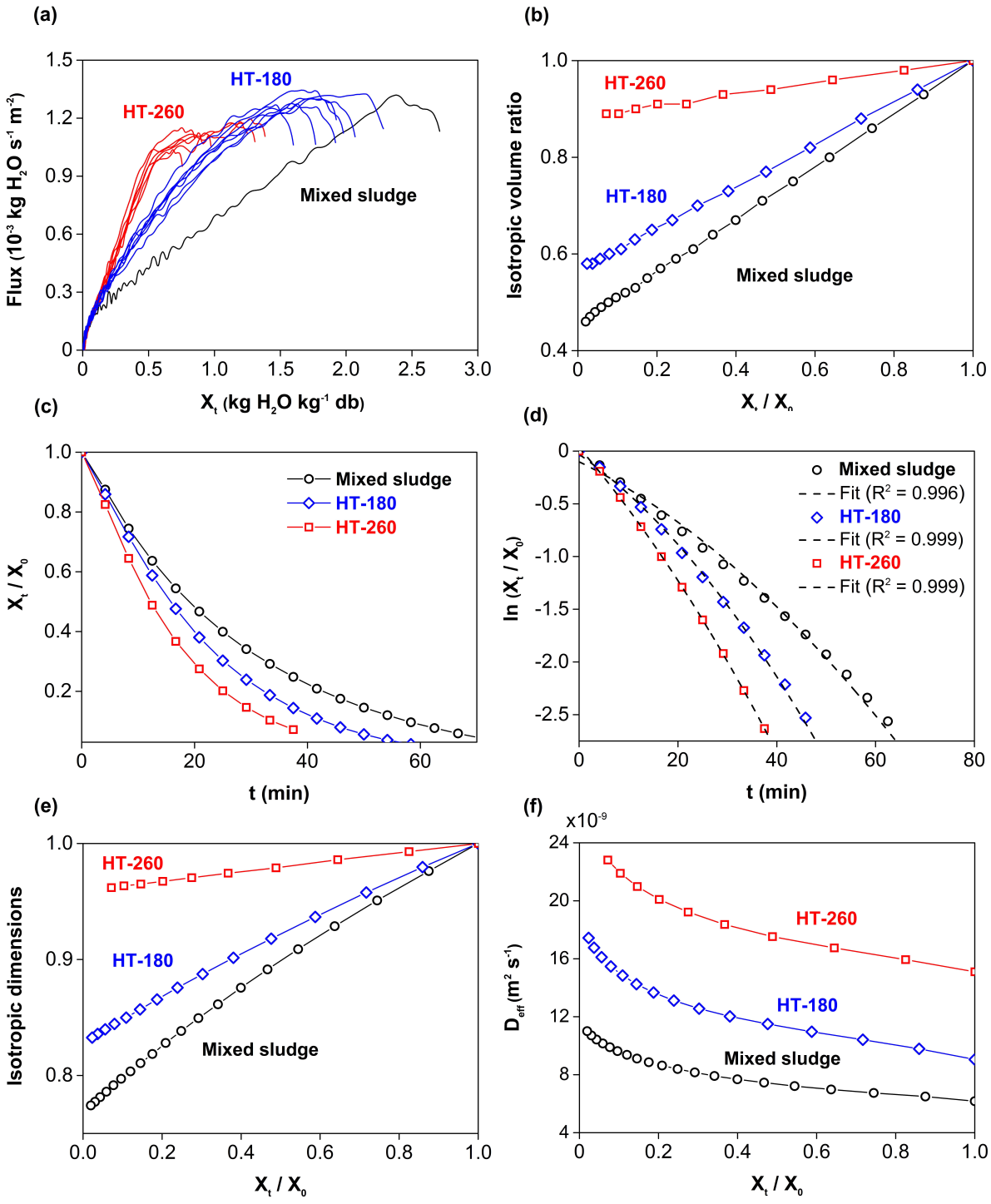

Fig. 3: a) Drying flux; b) Isotropic volume ratios; c) Moisture ratios (X_t / X_0); d) Polynomial fit of ln (X_t / X_0); e) Isotropic dimension ratios; and f) Effective moisture diffusivities (10^{-9} m^2 s^{-1}) of sludge and hydrochar as a function of moisture ratio. *In a) only hydrochar samples produced at 180 and 260 °C and in b)-f) only three samples (untreated sludge and exp. no. 11 and 14, Table 1) and every 50th data point are shown for clarity.*

An accepted version of Mäkelä et al., Water Res 91 (2016) 11-18, available at:
http://dx.doi.org/10.1016/j.watres.2015.12.043.

Coded and range-scaled regression model coefficients for predicting the mean moisture diffusivity of hydrochar were determined and are illustrated in Fig. S1 (Supplementary Information). Both hydrothermal treatment temperature ($p < 0.01$) and transformed retention time ($p < 0.05$) were statistically significant in predicting the mean moisture diffusivity of hydrochar according to the model. No statistically significant relationship was found between mean moisture diffusivity and the dummy variables used for describing additive quality ($p > 0.05$). The F-test performed against model residuals indicated that the attained model was statistically significant on a $p < 0.01$ significance level (Table S1). In addition, the calculated R^2 value suggested that the acquired model explained a satisfactory 76% of variation in the determined mean diffusivities of hydrochar samples.

5. Discussion

As illustrated in Fig. 3a, hydrothermal treatment led to considerable differences in the drying behavior of sludge and hydrochar samples. The drying of untreated sludge began by a short, sharp heating period where the drying flux increased rapidly due to increase in sample temperature. The constant drying rate period generally controlled by vapor transfer at the air-solid interface and the rate of moisture removal could only be seen as a slight increase in drying flux at approximately 2.5 kg H_2O kg^{-1} db due to simultaneous sample shrinkage (Fig. 3b). On the contrary, drying was mainly governed by the falling rate period during which the drying flux decreased continuously with a decrease in sludge moisture content. This period likely began as surface moisture was sufficiently reduced and moisture was transported to the surface of the solid by capillary forces (Bennamoun et al., 2013; Mujumdar, 2007). Moisture diffusion caused by concentration gradients within the sample matrix and heat conduction are generally regarded as the controlling mechanisms (Léonard et al., 2002).

In the case of hydrochar the initial moisture contents were lower due to hydrothermal treatment and subsequent solid-liquid separation by filtering. Hydrothermal treatment increased the drying flux of hydrochar and respectively decreased the length of the falling rate period (Fig. 3a) most likely due to sludge cell breakage (Dawei et al., 2012). In addition, two different phases could be observed during the falling rate period, the phases being especially distinguishable at approximately 0.5 kg H_2O kg^{-1} db for samples treated at 260 °C. As discussed by Léonard et al. (2002), the first phase of the falling rate period is normally governed by decreasing drying air humidity at the air-solid interface due to heat and mass transfer limitations and simultaneous sample shrinkage. During the second phase sample shrinkage decreases or ceases entirely as the decreasing drying flux is almost entirely caused by internal heat and mass transfer limitations (Léonard et al., 2002). Our observations on sample shrinkage in Fig. 3b do not entirely support this description as they assume linear isotropic shrinkage measured before and after the drying experiments. However, it is more likely that a higher degree of

shrinkage occurred in the beginning of the drying process during the constant rate period and the first phase of the falling rate period (Fig. 3a) especially with hydrochar samples where different falling rate periods could be distinguished. As illustrated in Fig. 3b hydrothermal treatment decreased sample shrinkage and the effect of heat and mass transfer limitations based on an increased drying flux.

Moisture diffusivity coefficients are often determined based on a simplification of Fick's second law of diffusion assuming isotropic diffusion (Pacheco-Aguirre et al., 2014). As illustrated in Fig. 3f, the determined effective moisture diffusivities of sludge and hydrochar increased as a function of decreasing moisture content. As described by Fyhr and Kemp (1998), moisture diffusivity in solids is nearly constant at higher moisture contents but generally reaches a peak when no free moisture is left in the solid and the only remaining mechanisms for moisture transport are diffusion and convective vapour flow. However, the peak is generally followed by a notable decrease in diffusivity as the moisture content of the solid approaches zero. In our data the determined diffusivities turned towards zero at low moisture contents, but could not be observed in Fig. 3f as the drying data was preprocessed by excluding data points beyond 95% dry solids. This affected the coefficients attained by fitting a polynomial function to the experimental data, but ensured comparability of mean moisture diffusivities between different samples. Recently Gómez-de la Cruz et al. (2015) reported a modification for the determination of effective diffusivities by using a second order polynomial for describing moisture ratio as a function of time. The authors also showed increasing effective diffusivities as a function of decreasing moisture contents and increasing drying temperature for rigid olive stone. In our case the modification yielded R^2 values in the range 0.996-0.999 for sludge and hydrochar samples and was hence adopted (Fig. 3d). This method also allowed taking sample shrinkage into account by including a time dependent function for sample height. As illustrated in Fig. 3b and e considerable sample shrinkage occurred especially with untreated sludge and hydrochar from lower treatment temperatures. Shrinkage however decreased considerably with an increase in hydrothermal treatment temperature, which also increased effective diffusivity of hydrochar at lower moisture contents (Fig. 3f). Previously Zhao et al. (2014a) investigated the drying properties of hydrothermally treated paper sludge and reported effective diffusivities in the range $1.26\text{-}1.71 \cdot 10^{-9}$ $m^2\ s^{-1}$ for hydrochar treated at 180-260 °C for 30 minutes. The authors used drying temperatures of 30 °C, did not take shrinkage into account and used a linear model for describing the evolution of moisture ratio as a function of drying time. However, Bennamoun et al. (2013) reported a diffusivity difference of 106-134% if shrinkage is not taken into account during laboratory drying experiments on municipal sludge.

The attained regression model indicated that hydrothermal treatment temperature was 1.6 times as important as transformed retention time in controlling the mean moisture diffusivity of hydrochar (Fig. S1). As the experimental variables were coded and range-scaled their effects could be compared

within the original design range. In addition, the dummy variables used for describing the effect of acid and base additions suggested that the use of NaOH or HCl did not significantly affect the mean moisture diffusivity of hydrochar ($p > 0.05$). Previously the effect of process conditions have mainly been investigated in terms of solid fuel properties and yields of attained hydrochar. Although it is currently well known that temperature mainly governs biomass decomposition in hydrothermal media, retention time has also been found significant for the fuel properties of hydrochar produced from algae and municipal and industrial sludge (Danso-Boateng et al., 2015; Heilmann et al., 2011; Mäkelä et al., 2015; Xu et al., 2013). In addition, Lynam et al. (2011) found that organic acid additions enhanced cellulose dissolution and respectively decreased hydrochar yield during hydrothermal treatment of lignocellulosic biomass. Furthermore, Lu et al. (2014) reported statistically different solid yields of hydrothermally treated cellulose in NaOH and HCl due to changes in reaction kinetics. In this work the mean diffusivities of hydrochar were higher with the use of H_2O than with NaOH or HCl, but the overall differences were not statistically significant (Fig. S1). Liquid pH values measured after the hydrothermal experiments were in the range 4.9-5.5 and correlated only with treatment temperature ($p < 0.01$) and retention time ($p < 0.05$). This suggests that the strength of used additives were not sufficient to significantly change reaction conditions and were neutralized likely due to the formation of organic acids during biomass decomposition under hydrothermal conditions (Berge et al., 2011; Weiner et al., 2014). Equivalent hydroxide and hydronium ion concentrations from NaOH and HCl have previously been used for simulating different pH environments in municipal and industrial waste streams (Lu et al., 2014). In addition, equivalent hydroxide concentrations from KOH have been reported to lead to decreased surface area and pore volume of hydrothermally treated wheat straw (Reza et al., 2015) which could have practical implications for the drying behavior of hydrochar. Besides evaluating the effect of process conditions the attained model coefficients enable prediction of novel observations, which is very useful for illustrating the behavior of mean diffusivity of hydrochar within the design range. Respective contours were hence calculated based on hydrothermal treatment temperature and retention time in NaOH, H_2O and HCl and are shown in Fig. 4. The linear increase in mean diffusivity as a function reaction temperature and retention time could easily be observed and was more pronounced with NaOH or H_2O compared to HCl. As an example, hydrothermal treatment at 220 °C with a retention time of 1.5 h in H_2O would be expected to increase the mean effective diffusivity of sludge to $18.2 \pm 5.80 \cdot 10^{-9}$ m^2 s^{-1} with 95% certainty. According to our better knowledge this is the first time the effect and statistical significance of hydrothermal treatment conditions on the mean moisture diffusivity and drying behavior of sludge have been reported. Once these effects are known, the mean diffusivity of sludge can be predicted within the design thus allowing control of respective drying properties based on hydrothermal treatment conditions. This information is vital for optimizing hydrothermal treatment and subsequent drying processes for this feedstock.

An accepted version of Mäkelä et al., Water Res 91 (2016) 11-18, available at:
http://dx.doi.org/10.1016/j.watres.2015.12.043.

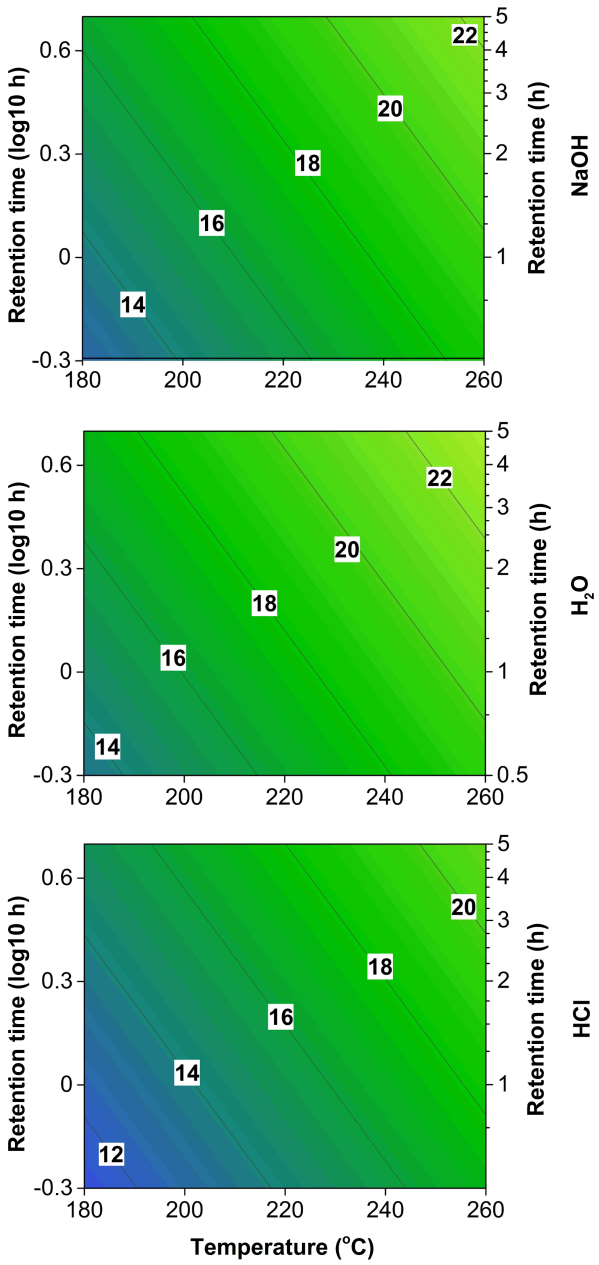

Fig. 4: Predicted mean effective moisture diffusivity (10^{-9} m^2 s^{-1}) of hydrochar as a function of reaction temperature (°C) and retention time (h) in NaOH, H_2O and HCl.

Conclusions

Hydrothermal treatment enhanced the drying properties and increased the effective moisture diffusivity of sludge. Drying of untreated sludge was governed by the falling rate period where drying flux decreased continuously as a function of sludge moisture content due to heat and mass transfer limitations and sample shrinkage. Hydrothermal treatment increased the drying flux of sludge

hydrochar and decreased the effect of internal heat and mass transfer limitations and sample shrinkage especially at higher treatment temperatures. The determined effective moisture diffusivities increased as a function of decreasing moisture content and a statistically significant difference was found between the mean diffusivity of untreated sludge and sludge hydrochar. The attained regression model indicated that treatment temperature controlled the mean moisture diffusivity of hydrochar as the effects of NaOH and HCl were found statistically insignificant. The presented results enabled prediction of sludge drying properties through mean moisture diffusivity based on hydrothermal treatment conditions.

Acknowledgements

The contributions of Markus Segerström and Gunnar Kalén from the Swedish University of Agricultural Sciences in sample processing are deeply appreciated. This work was performed in cooperation with SCA Obbola AB with partial funding from SP Processum AB.

References

Alatalo, S.-M., Repo, E., Mäkilä, E., Salonen, J., Vakkilainen, E., Sillanpää, M., 2013. Adsorption behavior of hydrothermally treated municipal sludge & pulp and paper industry sludge. Bioresource Technology 147, 71-76. doi: 10.1016/j.biortech.2013.08.034.

Bennamoun, L., Crine, M., Léonard, A., 2013. Convective drying of wastewater sludge: introduction of shrinkage effect in mathematical modeling. Drying Technology 31, 643-654. doi: 10.1080/07373937.2012.752743.

Berge, N.D., Ro, K.S., Mao, J., Flora, J.R.V., Chappell, M.A., Bae, S., 2011. Hydrothermal carbonization of municipal waste streams. Environmental Science and Technology 45, 5696-5703. doi: 10.1021/es2004528.

Crank, J. The Mathematics of Diffusion (2nd ed.). Oxford University Press: London, 1975, 414 pp.

Danso-Boateng, E., Shama, G., Wheatley, A.D., Martin, S.J., Holdich, R.G., 2015. Hydrothermal carbonisation of sewage sludge: effect of process conditions on product characteristics and methane production. Bioresource Technology 177, 318-327. doi: 10.1016/j.biortech.2014.11.096.

Dawei, M., Zili, J., Yoshikawa, K., Hongyan, M., 2012. The effect of operation parameters on the hydrothermal drying treatment. Renewable Energy 42, 90-94. doi: 10.1016/j.renene.2011.09.011.

Fraikin, L., Contribution à l'étude du séchage convectif de boues de station d'épuration et des émissions gazeuses associées, University of Liège, Department of Chemical Engineering, 2012.

Fyhr, C., Kemp, I.C., 1998. Comparison of different drying kinetics models for single particles. Drying Technology 16, 1339-1369. doi: 10.1080/07373939808917465.

Gerlach, R.W., Dobb, D.E., Raab, G.A., Nocerino, J.M., 2002. Gy sampling theory in environmental studies. 1. Assessing soil splitting protocols. Journal of Chemometrics 16, 321-328. doi: 10.1002/cem.705.

Gómez-de la Cruz, F.J., Palomar-Carnicero, J.M., Casanova-Peláez, P.J., Cruz-Peragón, F., 2015. Experimental determination of effective moisture diffusivity during the drying of clean olive stone: dependence of temperature, moisture content and sample thickness. Fuel Processing Technology 137, 320-326. doi: 10.1016/j.fuproc.2015.03.018.

Heilmann, S.M., Jader, L.R., Sadowsky, M.J., Schendel, F.J., von Keitz, M.G., Valentas, K.J., 2011. Hydrothermal carbonization of distiller's grains. Biomass and Bioenergy 35, 2526-2533. doi: 10.1016/j.biombioe.2011.02.022.

Kruse, A., Funke, A., Titirici, M.-M., 2013. Hydrothermal conversion of biomass to fuels and energetic materials. Current Opinion in Chemical Biology 17, 515-521. doi: 10.1016/j.cbpa.2013.05.004.

Léonard, A., Blacher, S., Marchot, P., Crine, M., 2002. Use of X-ray microtomography to follow the convective heat drying of wastewater sludges. Drying Technology 20, 1053-1069. doi: 10.1081/DRT-120004013.

Léonard, A., Blacher, S., Marchot, P., Pirard, J.P., Crine, M., 2004. Measurement of shrinkage and cracks associated to convective drying of soft materials by X-ray microtomography. Drying Technology 22, 1695-1708. doi: 10.1081/DRT-200025629.

Léonard, A., Meneses, E., Le Trong, E., Salmon, T., Marchot, P., Toye, D., Crine, M., 2008. Influence of back mixing on the convective drying of residual sludges in a fixed bed. Water Research 42, 2671-2677. doi: 10.1016/j.watres.2008.01.020.

Li, J., Bennamoun, L., Fraikin, L., Salmon, T., Toye, D., Schreinemachers, R., Léonard, A., 2014. Analysis of the shrinkage effect on mass transfer during convective drying of sawdust/sludge mixtures. Drying Technology 32, 1706-1717. doi: 10.1080/07373937.2014.924136.

Libra, J.A., Ro, K.S., Kammann, C., Funke, A., Berge, N.D., Neubauer, Y., Titirici, M.-M., Fühner, C., Bens, O., Kern, J., Emmerich, K.-H., 2011. Hydrothermal carbonization of biomass residuals: a comparative review of the chemistry, processes and applications of wet and dry pyrolysis. Biofuels 2, 71-106. doi: 10.4155/BFS.10.81.

Lu, X., Flora, J.R.V., Berge, N.D., 2014. Influence of process water quality on hydrothermal carbonization of cellulose. Bioresource Technology 154, 229-239. doi: 10.1016/j.biortech.2013.11.069.

Lynam, J.G., Coronella, C.J., Yan, W., Reza, M.T., Vasquez, V.R., 2011. Acetic acid and lithium chloride effects on hydrothermal carbonization of lignocellulosic biomass. Bioresource Technology 102, 6192-6199. doi: 10.1016/j.biortech.2011.02.035.

Mahmood, T., Elliott, A., 2006. A review of secondary sludge reduction technologies for the pulp and paper industry. Water Research 40, 2093-2112. doi: 10.1016/j.watres.2006.04.001.

Mäkelä, M., Benavente, V., Fullana, A., 2015. Hydrothermal carbonization of lignocellulosic biomass: effect of process conditions on hydrochar properties. Applied Energy 155, 576-584. doi: 10.1016/j.apenergy.2015.06.022.

Mowla, D., Tran, H.N., Grant Allen, D., 2013. A review of the properties of biosludge and its relevance to enhanced dewatering processes. Biomass and Bioenergy 58, 365-378. doi: 10.1016/j.biombioe.2013.09.002.

Mujumdar, A.S., Principles, Classification and Selection of Dryers. In: Handbook of Industrial Drying (3rd ed.), A. S. Mujumdar (Eds.), CRC Press: Boca Raton; 2007, pp. 4-32.

Myers, R.H., Montgomery, D.C., Anderson-Cook, C.M., Experimental Designs for Fitting Response Surfaces - II. In: Response Surface Methodology: Process and Product Optimization Using Designed Experiments (3rd ed.), R. H. Myers, D. C. Montgomery and C. M. Anderson-Cook (Eds.), John Wiley & Sons, Inc.: Hoboken; 2009, pp. 349-416.

Pacheco-Aguirre, F.M., Ladrón-González, A., Ruiz-Espinosa H, García-Alvarado, M.A., Ruiz-López, I.I., 2014. A method to estimate anisotropic diffusion coefficients in cylindrical solids: application to the drying of carrot. Journal of Food Engineering 125, 24-33. doi: 10.1016/j.jfoodeng.2013.10.015.

Peterson, A.A., Vogel, F., Lachance, R.P., Fröling, M., Antal Jr., M.M., Tester, J.W., 2008. Thermochemical biofuel production in hydrothermal media: a review of sub- and supercritical water technologies. Energy & Environmental Science 1, 32-65. doi: 10.1039/b810100k.

Reza, M.T., Rottler, E., Herklotz, L., Wirth, B., 2015. Hydrothermal carbonization (HTC) of wheat straw: influence of feedwater pH prepared by acetic acid and potassium hydroxide. Bioresource Technology 182, 336-344. doi: 10.1016/j.biortech.2015.02.024.

Sevilla, M., Fuertes, A.B., 2009. The production of carbon materials by hydrothermal carbonization of cellulose. Carbon 47, 2281-2289. doi: 10.1016/j.carbon.2009.04.026.

Stoica, A., Sandberg, M., Holby, O., 2009. Energy use and recovery strategies within wastewater treatment and sludge handling at pulp and paper mills. Bioresource Technology 100, 3497-3505. doi: 10.1016/j.biortech.2009.02.041.

Titirici, M.-M., Antonietti, M., 2010. Chemistry and material options of sustainable carbon materials made by hydrothermal carbonization. Chemical Society Reviews 39, 103-116. doi: 10.1039/b819318p.

Vaxelaire, J., Cézac, P., 2004. Moisture distribution in activated sludges: a review. Water Research 38, 2215-2230. doi: 10.1016/j.watres.2004.02.021.

Wang, L., Zhang, L., Li, A., 2014. Hydrothermal treatment coupled with mechanical expression at increased temperature for excess sludge dewatering: influence of operating conditions and process energetics. Water Research 65, 85-97. doi: 10.1016/j.watres.2014.07.020.

Weiner, B., Poerschmann, J., Wedwitschka, H., Koehler, R., Kopinke, F.-D., 2014. Influence of process water reuse on the hydrothermal carbonization of paper. ACS Sustainable Chemistry & Engineering 2, 2165-2171. doi: 10.1021/sc500348v.

Xu, Q., Qian, Q., Quek, A., Ai, N., Zeng, G., Wang, J., 2013. Hydrothermal carbonization of macroalgae and the effects of experimental parameters on the properties of hydrochars. ACS Sustainable Chemistry & Engineering 1, 1092-1101. doi: 10.1021/sc400118f.

Yoshikawa, K., Prawisudha, P., Hydrothermal Treatment of Municipal Solid Waste for Producing Solid Fuel. In: Application of Hydrothermal Reactions to Biomass Conversion (1st ed.), F. Jin (Eds.), Springer: Heidelberg; 2014a, pp. 355-383.

Yoshikawa, K., Prawisudha, P., Sewage Sludge Treatment by Hydrothermal Process for Producing Solid Fuel. In: Application of Hydrothermal Reactions to Biomass Conversion (1st ed.), F. Jin (Eds.), Springer: Heidelberg; 2014b, pp. 385-409.

An accepted version of Mäkelä et al., Water Res 91 (2016) 11-18, available at:
http://dx.doi.org/10.1016/j.watres.2015.12.043.

Zhao, P., Ge, S., Ma, D., Areeprasert, C., Yoshikawa, K., 2014a. Effect of hydrothermal pretreatment on convective drying characteristics of paper sludge. ACS Sustainable Chemistry & Engineering 2, 665-671. doi: 10.1021/sc4003505.

Zhao, P., Shen, G., Ge, S., Chen, Z., Yoshikawa, K., 2014b. Clean solid biofuel production from high moisture content waste biomass employing hydrothermal treatment. Applied Energy 131, 345-367. doi: 10.1016/j.apenergy.2014.06.038.

The author has requested enhancement of the downloaded file. All in-text references underlined in blue are linked to publications on ResearchGate.